Zeptosecond High Harmonic keV X-Ray Waveforms Driven by Midinfrared Laser Pulses

C. Hernández-García,[1,3,*] J. A. Pérez-Hernández,[2] T. Popmintchev,[3] M. M. Murnane,[3] H. C. Kapteyn,[3] A. Jaron-Becker,[3] A. Becker,[3] and L. Plaja[1]

[1]*Grupo de Investigación en Óptica Extrema, Universidad de Salamanca, E-37008 Salamanca, Spain*
[2]*Centro de Láseres Pulsados (CLPU), Parque Científico, 37185 Villamayor, Salamanca, Spain*
[3]*JILA and Department of Physics, University of Colorado at Boulder, Boulder, Colorado 80309-0440, USA*

(Received 30 January 2013; published 18 July 2013)

We demonstrate theoretically that the temporal structure of high harmonic x-ray pulses generated with midinfrared lasers differs substantially from those generated with near-infrared pulses, especially at high photon energies. In particular, we show that, although the total width of the x-ray bursts spans femtosecond time scales, the pulse exhibits a zeptosecond structure due to the interference of high harmonic emission from multiple reencounters of the electron wave packet with the ion. Properly filtered and without any compensation of the chirp, regular subattosecond keV waveforms can be produced.

DOI: 10.1103/PhysRevLett.111.033002 PACS numbers: 32.30.Rj, 32.80.Fb, 42.65.Ky

The quest to capture dynamical processes with ever finer time resolution on time scales associated with processes in atoms, molecules, and more recently of electrons is one of the motivations behind the development of ultrashort light pulses [1–11]. Over a decade ago, the femtosecond barrier ($1\ \text{fs} = 10^{-15}$ s) was broken by generating isolated attosecond pulses and pulse trains of high harmonics of a fundamental Ti:sapphire laser [12–17]. The shortest light pulses to date are produced as a broad coherent spectrum of high harmonic radiation that results from the extreme nonlinear interaction of intense femtosecond lasers with atomic or molecular gases. Attosecond pulses and pulse trains are then obtained by using a filter to select the highest spectral contributions, which are spontaneously phase locked [12], that support pulse durations <100 as [16,18]. Isolation of a single attosecond pulse from the train has also been reported recently [19]. From the uncertainty principle, the minimum pulse duration that can be achieved using this scheme scales inversely with the width of the coherent spectrum.

At the single atom level, the underlying mechanism from which high-energy photons are generated is surprisingly simple [20,21]: an electron is first removed from the atom by the laser field and then driven back to the parent ion when the sign of the field reverses. Upon rescattering, the electron can recombine, releasing its kinetic energy in the form of high-order harmonic radiation. Since the maximum return energy of the electron scales with the square of the laser wavelength, it has long been understood that the maximum harmonic photon energy should quickly increase using longer-wavelength driving laser pulses [22]. However, at this single atom level, it is also known that the probability of rescattering and, hence, the efficiency of high-order harmonic generation (HHG) rapidly decreases with increasing driver laser wavelength. Fortunately, this decrease in the single-atom efficiency can be balanced by favorable phase matching at high pressure and long interaction length in the keV photon regime [23–27]. Thus, bright coherent keV high harmonic x-rays can be generated, provided midinfrared (mid-IR) driving laser pulses are used. Both experiment and theory confirm that the bandwidth of high harmonic x-ray emission driven by mid-IR lasers is enormous—spanning keV bandwidths that, in the Fourier limit, are sufficient to support single-cycle few attosecond pulses [26,27]. However, theoretical predictions also show that this limit is currently not reached, because the harmonics emerge with a large chirp leading to longer bursts, of femtosecond duration [27]. Although the predicted phase of the HHG emission is smooth, compensation of this attochirp in order to generate few attosecond (or even subattosecond) pulses would be challenging.

In this Letter, we present a new and realistic route for breaking the attosecond barrier that is very attractive in its simplicity because it does not require that the chirp of the x-ray bursts is compensated. Our calculations show that the temporal structure of high harmonic x-ray pulses generated using mid-IR lasers differs substantially from those generated using near-infrared lasers, especially at high photon energies. In particular, we show that although the total temporal width of the x-ray bursts spans femtosecond time scales, they may exhibit a fine structure arising from the interference of x-ray emission due to multiple rescattering of the laser-driven electron wave packet with the ion. X-rays emitted as a result of the first rescattering can interfere with x-rays generated from electrons liberated during earlier half-cycles of the laser field that then reencounter the ion multiple times (see Fig. 1) [28]. With the use of few-cycle long wavelength 9 μm lasers, these interferences form a regular high-contrast interference pattern with subattosecond durations. The waveform, which corresponds to a 1 fs long envelope modulated at up to 1.3 exahertz frequencies, can be sculpted simply by using thin metal filters of various thickness and by

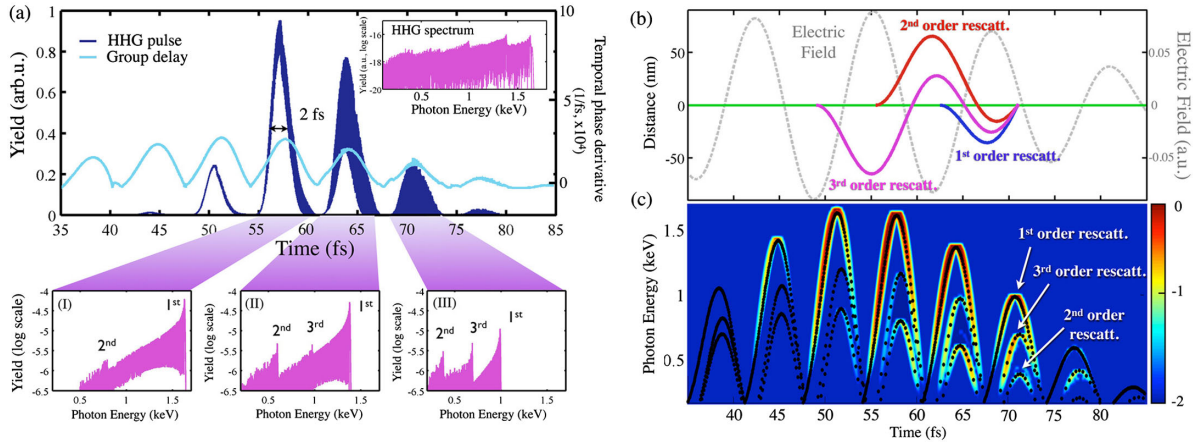

FIG. 1 (color online). (a) Envelope of the x-ray bursts (dark blue line) and group delay (light blue line) obtained using a 3.9 μm wavelength laser. The HHG spectrum is shown in the inset, whereas in the panels below the spectral content of each burst is shown. (b) Schematic of the driving field and an example of the interfering trajectories contributing to the fs burst at 71 fs. (c) Time-frequency analysis (logarithmic scale). The dotted lines represent classical calculations of the electronic rescattering energies of trajectories with different rescattering orders.

adjusting the pulse duration and carrier-envelope phase of the driving laser.

Calculating high-harmonic spectra driven by mid-IR lasers is a challenging task, because the excursion of the electron wave packet in the laser field scales with the square of the laser wavelength (λ). For very long wavelength driving lasers, calculations are time consuming and challenging even for the single atom case, whereas calculations including propagation are beyond state-of-the-art theory. We use the recently developed SFA+ approach [29], which is an extension of the conventional strong field approximation [30–33] (see the Supplemental Material [34]). Figure 1 shows the results of an SFA+ calculation for high harmonics from helium driven by a laser of wavelength $\lambda = 3.9\ \mu$m and peak intensity 3.6×10^{14} W/cm^2 [similar to the recent demonstration of efficient generation of keV harmonics [27]]. The laser pulse is of the form $\sin^2(\pi t/2\tau_p)\sin(2\pi ct/\lambda)$ with pulse duration (FWHM) $\tau_p = 37.4$ fs (2.9 cycles). The high-frequency part of the spectrum, assuming that the harmonics pass through a 0.1 μm thick Al filter, clearly extends into the keV region [see inset in Fig. 1(a)]. The envelope of the corresponding electromagnetic field, which consists of a carrier wave at 1 keV photon energy, is represented in Fig. 1(a) (dark blue line: intensity, light blue line: phase). The results show that the x-ray emission is overall composed of bursts with temporal widths of about 2 fs. This temporal structure has the same physical origin as the attosecond pulse trains obtained using near-infrared laser wavelengths [35–39]. The long durations of the bursts are a consequence of the increased attochirp associated to the wider time interval in which energetic electron recollisions take place for longer driving laser wavelengths. Interestingly, the attochirp is predicted to decrease as λ^{-1}, which for a fixed HHG bandwidth would correspond to shorter x-ray pulses as we go to longer mid-IR laser wavelengths [40]. However, the generated phase-matched HHG bandwidth increases as $\lambda^{1.7}$ [25,26,41], which effectively leads to the emission of chirped x-ray bursts of femtosecond durations. To enhance visibility, the time resolution for the phase derivative has been chosen to average the additional fast oscillations that appear in the pulse train envelope, which will be discussed below. Therefore, the slope of the phase derivative contains coarse-grained information of the pulse chirp, which is regular [27] and is well explained by the temporal distribution of the short and long trajectories at the first recollision of the electron wave packet with the parent ion.

Most interesting is the fine structure of super-high-frequency oscillations that appears on some of the femtosecond HHG bursts. These structures are not observed using near-IR driving laser wavelengths around 0.8 μm and only appear when mid-IR driving fields are used. In our simulations, they appear gradually during the interaction and mainly influence the femtosecond x-ray bursts generated on the trailing part of the mid-IR pulse. As we will show below, the increasing contrast of the oscillations leads to the splitting of these femtosecond bursts into waveforms of a few attoseconds [or even hundreds of zeptoseconds (zs)] in duration.

The physics underlying these high-frequency modulations can be explained with the aid of the time-frequency analysis shown in Fig. 1(c). This plot shows the correlation of the HHG emission time with energy and, superimposed, the kinetic energy of the electrons at the moment of rescattering resulting from a classical trajectory analysis (dots). The three series of dots correspond to HHG emission from the first, second, or third consecutive rescatterings of the different electron trajectories with the parent ion. Examples of the classical trajectories leading to the three rescatterings are shown in Figure 1(b) for the HHG emission at 71 fs. The appearance of a fine structure in the

x-ray pulses is connected with the increase in relative strength of the HHG emission from the second and third rescatterings of the electron wave packet with the ion, as the driving laser wavelength is increased. Interference structures will become significant if the relative weights of HHG emission from the first and subsequent rescatterings are comparable. This occurs on the trailing edge of the laser pulse, where the efficiency loss associated with electron wave packet spreading for the second and third rescattering events is compensated by the higher ionization rate present when that electron is liberated into the continuum (which is closer to the peak of the mid-IR laser pulse). The different contributions to the multiple rescatterings are shown in the lower panels in Fig. 1(a), where we plot the spectral content of each fs burst. Note that the relevance of higher-order rescatterings for strong-field processes at longer wavelengths has been recently described in other contexts as well [28,40], although the possibility of harnessing the resulting interferences to manipulate the temporal emission of HHG was not realized.

Next, we show that the contrast due to HHG emission from interfering multiple rescattering events is significant enough to fully modulate the femtosecond x-ray bursts into a waveform of extremely short keV modulations, in some cases with attosecond and even subattosecond durations. To this end, we present in Fig. 2(a) the detailed structure of one of the femtosecond x-ray bursts originating at the tail of the mid-IR pulse. The temporal structures of the bursts obtained by using Al filters of different thicknesses [Fig. 2(c)] 0.1 μm, [Fig. 2(d)] 0.5 μm, and [Fig. 2(e)] using a 0.1 μm Al filter combined with an artificial high pass filter are compared with each other. The results clearly reveal the full modulation of the femtosecond burst into a waveform of beats of about 5 as in duration for this particular case.

Note that the beating structure is not regular [Fig. 2(c)] if there are HHG contributions from multiple rescattering processes. A more regular waveform can be obtained by increasing the thickness of the Al filter such that only the contributions of two rescatterings can interfere [Fig. 2(d)]. As expected for an interference pattern, the time between two consecutive bursts is given by $T = 2\pi/\Delta E$, where ΔE is the energy difference between the two dominant energetic contributions (here arising from the first and the third rescattering). Finally, suppression of all but the first rescattering events [Fig. 2(e)] leads to the disappearance of the fine structure, which unequivocally demonstrates that the interference effects are the origin for the attosecond fine structure in the femtosecond x-ray bursts.

We can now identify two conditions for the generation of atto- or zeptosecond waveforms using this approach: (i) the interference of two—*and only two*—electron wave packet rescattering events in order to form a regular modulation, and (ii) comparable strengths of the two contributions to the HHG emission in order to achieve good contrast. Both requirements can be met using few-cycle mid-IR driven pulses—even without tailoring using filters [as done in Fig. 2(d)]. The short duration of the driver pulse acts as a

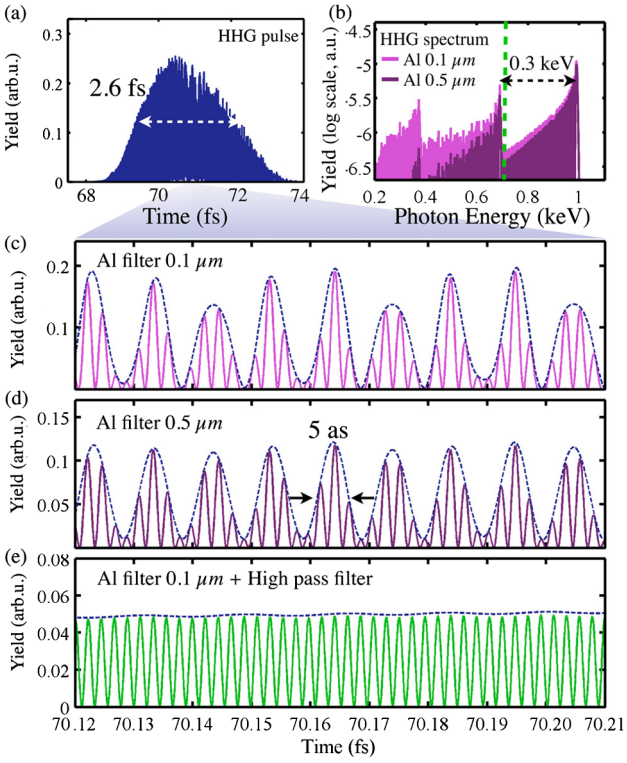

FIG. 2 (color online). (a) Detailed structure of an x-ray burst from the tailing edge of the keV pulse train shown in Fig. 1. The spectrum of the selected burst is shown in (b) for Al filters of 0.1 and 0.5 μm thickness. Plots (c) and (d) show a magnification of the temporal structure for the two Al filters, respectively, whereas (e) corresponds to the x-ray field obtained by selecting only the highest frequency contributions to the spectra.

temporal window, restricting the number of rescattering events, while their relative efficiency can be controlled using the carrier-envelope offset (see the Supplemental Material [34]). With this understanding, using classical trajectory analysis we perform predictions for the width of the beats in the waveform ($T/2$) as a function of the wavelength of a 1.5-cycle (FWHM) driver laser in Fig. 3(a). The intensities of the driver pulses are chosen to match those for which optimal phase matching is observed experimentally [41]. Our predictions show that the attosecond barrier will be broken for mid-IR wavelengths of about 7.7 μm.

For our simulations, we considered a driving laser field of the form $\sin^2(\pi t/2\tau_p)\sin(2\pi ct/\lambda + \phi_{\mathrm{CEO}})$ with wavelength $\lambda = 9\,\mu$m, intensity 3.4×10^{14} W/cm^2, pulse duration $\tau_p = 43$ fs (FWHM), and carrier-envelope offset $\phi_{\mathrm{CEO}} = -\pi/8$ [see inset on the upper left of Fig. 3(b)]. The results for the generated HHG spectrum (inset on lower left) and the envelope of the electromagnetic field, after transmission through an 0.2 μm thick Al filter, are shown in Fig. 3(b). There are two femtosecond bursts emitted, and the second burst is fully modulated into a zs waveform. In comparison to a 4 μm driver laser (shown in Fig. 1), for a 9 μm driver laser, the spectral cutoff increases to 8 keV, whereas the number of x-ray bursts

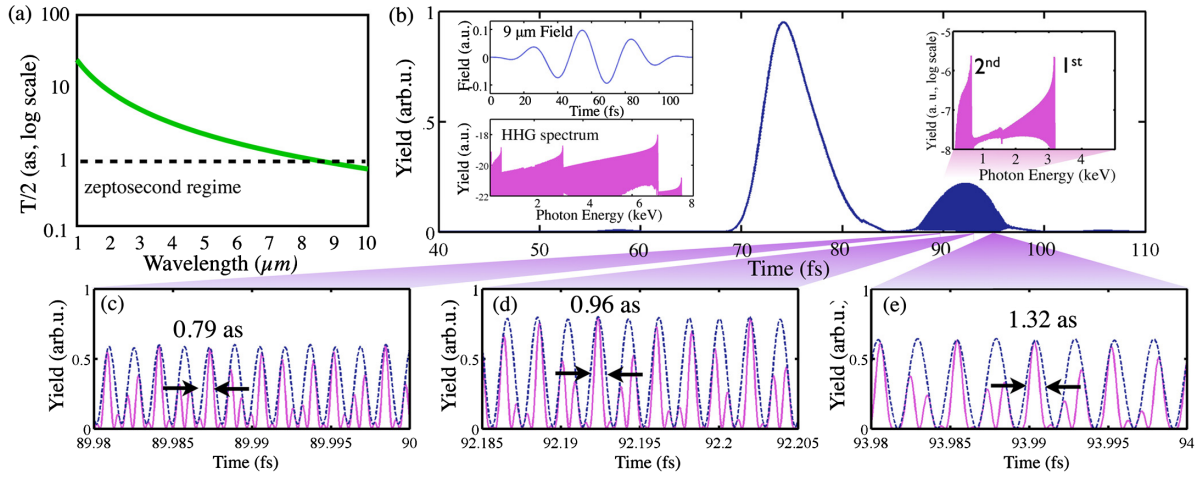

FIG. 3 (color online). (a) Predictions for the width of each keV beat in the waveform ($T/2$) as a function of the laser wavelength. (b) Envelope of the x-ray bursts obtained from a 1.5-cycle mid-IR pulse with wavelength $\lambda = 9\ \mu$m. Left insets: electric field of the driving pulse and high harmonic spectrum. Right inset: spectral content of the second fs burst. Panels (c)–(e) detail the fine temporal structure of the second fs burst: (solid pink line) absolute value of the electric field, and (dashed blue line) field envelope.

emitted is smaller, as expected due to the few number of cycles in the laser field. Our method shows that it is possible to control the contrast and the duration of the zs waveform by changing the carrier-envelope offset of the laser pulse (see the Supplemental Material [34]). In Fig. 3(b) the value of the carrier-envelope offset of the laser pulse is chosen to optimize the relative weight of the two rescattering contributions for the second burst (inset on right) and, hence, the contrast of the modulations in the waveform. Thus, the HHG emission has interferences from only two rescattering events, each with comparable efficiency, and as a result, a zeptosecond waveform is formed [see Figs. 3(c)–3(e)]. The atto-to-zepto chirp associated with the temporal distribution of each of the two rescatterings leads to the emission of shorter keV beats (0.72 as) on the leading edge [Fig. 3(c)] and longer beats (1.32 as) on the trailing edge of the burst [Fig. 3(e)].

A complete simulation of the HHG process needs to include propagation in order to take into account phase-matching effects. For such long wavelengths (9 μm), computing HHG propagation is not feasible using current state-of-the-art theory. However, we have computed one-dimensional propagation [42] for a 2 μm laser source over a distance of half a millimeter (see the Supplemental Material [34]). Our results confirm that the modulations in the attosecond regime are preserved, and thus, we expect that the atto or zepto modulations are preserved for longer driving wavelengths.

We emphasize that the present scheme for generating zs waveforms does not rely on compensating the attochirp but rather makes use of the fact that the relative strength of HHG emission due to multiple rescatterings of the electron wave packet becomes comparable using mid-IR laser wavelengths. By controlling the duration and carrier-envelope offset of $>7\ \mu$m driving laser pulses, the generation of a regular waveform consisting of modulations with zeptosecond duration is realizable. Although one can expect to generate even shorter x-ray oscillations at wavelengths much longer than 9 μm, one needs to consider that at those wavelengths, the drift associated with the magnetic term of the Lorentz force would lead to a drift of the electron trajectory away from the parent ion that becomes comparable to the large expansion of the free wave packet and, therefore, to a reduction of the harmonic yield (see the Supplemental Material [34]).

In conclusion, we have identified a route to generate zeptosecond waveforms, applicable to keV high harmonic x-rays driven by mid-IR lasers and without any compensation of the attochirp. Our numerical results have shown that the keV radiation exhibits an ultrashort fine structure due to the interference of x-ray emissions from multiple scattering events. This mechanism is predicted to lead to the generation of a regular waveform in the zeptosecond time scale by controlling the duration and carrier-envelope offset of $>7\ \mu$m driving laser pulses.

C. H.-G. acknowledges support by a Marie Curie International Outgoing Fellowship within the EU Seventh Framework Programme for Research and Technological Development (2007–2013), under REA grant agreement No. 328334. C. H.-G., J. A. P.-H., and L. P. acknowledge support from Spanish MINECO (CSD 2007-00013 and FIS 2009-09522). A. B., M. M. M. and H. C. K. acknowledge support from the United States Air Force Office of Scientific Research through the MURI "Mathematical Modeling and Experimental Validation of Ultrafast Nonlinear Light-Matter Coupling associated with Filamentation in Transparent Media" (Grant No. FA9550-10-1-0561) and by the National Science Foundation (Grant No. 1125844). A.J.-B. was supported by the National Science Foundation under Grant Nos. 1125844 and 1068706.

*carloshergar@usal.es

[1] M. Asaki, C. P. Huang, D. Garvey, J. Zhou, H. C. Kapteyn, and M. M. Murnane, Opt. Lett. **18**, 977 (1993).

[2] H. Niikura, F. Légaré, R. Hasbani, A. D. Bandrauk, M. Yu. Ivanov, D. M. Villeneuve, and P. B. Corkum, Nature (London) **417**, 917 (2002).

[3] S. Tanaka and S. Mukamel, Phys. Rev. Lett. **89**, 043001 (2002).

[4] A. Baltuška, Th. Udem, M. Uiberacker, M. Hentschel, E. Goulielmakis, Ch. Gohle, R. Holzwarth, V. S. Yakovlev, A. Scrinzi, T. W. Hänsch, and F. Krausz, Nature (London) **421**, 611 (2003).

[5] J. Itatani, J. Levesque, D. Zeidler, H. Niikura, H. Pépin, J. C. Kieffer, P. B. Corkum, and D. M. Villeneuve, Nature (London) **432**, 867 (2004).

[6] S. Baker, J. S. Robinson, C. A. Haworth, H. Teng, R. A. Smith, C. C. Chirilă, M. Lein, J. W. G. Tisch, and J. P. Marangos, Science **312**, 424 (2006).

[7] E. Gagnon, P. Ranitovic, X. Tong, C. L. Cocke, M. M. Murnane, H. C. Kapteyn, and A. S. Sandhu, Science **317**, 1374 (2007).

[8] N. L. Wagner, A. Wuüest, I. P. Christov, T. Popmintchev, X. Zhou, M. M. Murnane, and H. C. Kapteyn, Proc. Natl. Acad. Sci. U.S.A. **103**, 13279 (2006).

[9] W. Li, X. Zhou, R. Lock, S. Patchkovskii, A. Stolow, H. C. Kapteyn, and M. M. Murnane, Science **322**, 1207 (2008).

[10] S. Baker, I. A. Walmsley, J. W. G. Tisch, and J. P. Marangos, Nat. Photonics **5**, 664 (2011).

[11] R. M. Lock, S. Ramakrishna, X. Zhou, H. C. Kapteyn, M. M. Murnane, and T. Seideman, Phys. Rev. Lett. **108**, 133901 (2012).

[12] I. P. Christov, M. M. Murnane, and H. C. Kapteyn, Phys. Rev. Lett. **78**, 1251 (1997).

[13] P. M. Paul, E. S. Toma, P. Breger, G. Mullot, F. Augé, Ph. Balcou, H. G. Muller, and P. Agostini, Science **292**, 1689 (2001).

[14] R. Kienberger, E. Goulielmakis, M. Uiberacker, A. Baltuška, V. Yakovlev, F. Bammer, A. Scrinzi, Th. Westerwalbesloh, U. Kleineberg, U. Heinzmann, M. Drescher, and F. Krausz, Nature (London) **427**, 817 (2004).

[15] G. Sansone, E. Benedetti, F. Calegari, C. Vozzi, L. Avaldi, R. Flammini, L. Poletto, P. Villoresi, C. Altucci, R. Velotta, S. Stagira, S. De Silvestri, and M. Nisoli, Science **314**, 443 (2006).

[16] E. Goulielmakis, M. Schultze, M. Hofstetter, V. S. Yakovlev, J. Gagnon, M. Uiberacker, A. L. Aquila, E. M. Gullikson, D. T. Attwood, R. Kienberger, F. Krausz, and U. Kleineberg, Science **320**, 1614 (2008).

[17] I. Thomann, A. Bahabad, R. Trebino, M. M. Murnane, and H. C. Kapteyn, Opt. Express **17**, 4611 (2009).

[18] K. Zhao, Q. Zhang, M. Chini, Y. Wu, X. Wang, and Z. Chang, Opt. Lett. **37**, 3891 (2012).

[19] H. Vincenti and F. Quéré, Phys. Rev. Lett. **108**, 113904 (2012).

[20] K. J. Schafer, B. Yang, L. F. DiMauro, and K. C. Kulander, Phys. Rev. Lett. **70**, 1599 (1993).

[21] P. B. Corkum, Phys. Rev. Lett. **71**, 1994 (1993).

[22] B. Shan and Z. Chang, Phys. Rev. A **65**, 011804 (2001).

[23] T. Popmintchev, M.-C. Chen, O. Cohen, M. E. Grisham, J. J. Rocca, M. M. Murnane, and H. C. Kapteyn, Opt. Lett. **33**, 2128 (2008).

[24] E. J. Takahashi, T. Kanai, K. L. Ishikawa, Y. Nabekawa, and K. Midorikawa, Phys. Rev. Lett. **101**, 253901 (2008).

[25] T. Popmintchev, M. C. Chen, A. Bahabad, M. Gerrity, P. Sidorenko, O. Cohen, I. P. Christov, M. M. Murnane, and H. C. Kapteyn, Proc. Natl. Acad. Sci. U.S.A. **106**, 10516 (2009).

[26] M. C. Chen, P. Arpin, T. Popmintchev, M. Gerrity, B. Zhang, M. Seaberg, D. Popmintchev, M. M. Murnane, and H. C. Kapteyn, Phys. Rev. Lett. **105**, 173901 (2010).

[27] T. Popmintchev, M. Chen, D. Popmintchev, P. Arpin, S. Brown, S. Ališauskas, G. Andriukaitis, T. Balčiunas, O. Mücke, A. Pugzlys, A. Baltuška, B. Shim, S. E. Schrauth, A. Gaeta, C. Hernández-García, L. Plaja, A. Becker, A. Jaroń-Becker, M. M. Murnane, and H. C. Kapteyn, Science **336**, 1287 (2012).

[28] D. D. Hickstein, P. Ranitovic, S. Witte, X. M. Tong, Y. Huismans, P. Arpin, X. Zhou, K. E. Keister, C. W. Hogle, B. Zhang, C. Ding, P. Johnsson, N. Toshima, M. J. J. Vrakking, M. M. Murnane, and H. C. Kapteyn, Phys. Rev. Lett. **109**, 073004 (2012).

[29] J. A. Pérez-Hernández, L. Roso, and L. Plaja, Opt. Express **17**, 9891 (2009).

[30] L. V. Keldysh, Zh. Eksp. Teor. Fiz. **47**, 1945 (1964) [Sov. Phys. JETP **20**, 1307 (1965)].

[31] F. H. M. Faisal, J. Phys. B **6**, L89 (1973).

[32] H. R. Reiss, Phys. Rev. A **22**, 1786 (1980).

[33] W. Becker, A. Lohr, M. Kleber, and M. Lewenstein, Phys. Rev. A **56**, 645 (1997).

[34] See Supplemental Material at http://link.aps.org/supplemental/10.1103/PhysRevLett.111.033002 for a detailed discussion of the SFA+ method, the control over the zs waveforms by changing the carrier-envelope offset, propagation effects, and the magnetic drift in HHG.

[35] P. Antoine, A. L'Huillier, and M. Lewenstein, Phys. Rev. Lett. **77**, 1234 (1996).

[36] M. B. Gaarde and K. J. Schafer, Phys. Rev. Lett. **89**, 213901 (2002).

[37] Y. Mairesse, A. de Bohan, L. J. Frasinski, H. Merdji, L. C. Dinu, P. Monchicourt, P. Breger, M. Kovačev, R. Taïeb, B. Carré, H. G. Muller, P. Agostini, and P. Saliéres, Science **302**, 1540 (2003).

[38] R. López-Martens, K. Varjú, P. Johnsson, J. Mauritsson, Y. Mairesse, P. Saliéres, M. B. Gaarde, K. J. Schafer, A. Persson, S. Svanberg, C. G. Wahlström, and A. L'Huillier, Phys. Rev. Lett. **94**, 033001 (2005).

[39] C. Hernández-García and L. Plaja, J. Phys. B **45**, 074021 (2012).

[40] J. Tate, T. Auguste, H. G. Muller, P. Salières, P. Agostini, and L. F. Di Mauro, Phys. Rev. Lett. **98**, 013901 (2007).

[41] T. Popmintchev, M. C. Chen, P. Arpin, M. M. Murnane, and H. C. Kapteyn, Nat. Photonics **4**, 822 (2010).

[42] C. Hernández-García, J. A. Pérez-Hernández, J. Ramos, E. Conejero Jarque, L. Roso, and L. Plaja, Phys. Rev. A **82**, 033432 (2010).